Studies on the Gust Response of a Wing
Part II. Response of a Two-Dimensional Elastic Wing

By

Hiroshi MAEDA* and Makoto KOBAYAKAWA**

(Received June 30, 1971)

In this report, the responses of an elastic wing to two-dimensional gusts were investigated.

The deformations of a two-dimensional elastic wing caused by gust were separated into two types, i. e., the bending mode and the torsional mode.

The gusts treated here were the sinusoidal gust and the random gust. In the case of sinusoidal gust, the modes of deformation were obtained both theoretically and experimentally. In the case of random gust, the power spectral functions and the frequency transfer functions were obtained experimentally. The frequency transfer functions obtained by theoretical calculations were also compared with the experimental values.

1. Introduction

In a previous report[1], we investigated the gust response of a two-dimensional rigid wing, both theoretically and experimentally. The term "gust" denotes the atmospheric velocity fluctuation normal to the forward velocity of the wing (or the direction of the uniform flow) ; two kinds of gust, that which fluctuates sinusoidally (sinusoidal gust) and that which fluctuates randomly (random gust), were treated.

In the present report, the responses of a two-dimensional elastic wing to sinusoidal and random gusts are discussed. Many reports have been published on the nonsteady aerodynamic problems of the elastic wing, for example, the flutter phenomena, but only a few reports have been published on the gust response of an elastic wing[2].

In this report, the forced oscillations of a wing induced by gusts were investigated. Generally, these oscillations are weak and the influences on the dynamic stability of an airplane are small, but sometimes resonance phe-

* Dept. of Aeronautical Engineering
** Kansai University

nomena are induced, and therefore, the research on forced oscillation is very important.

As the responses of an elastic wing to gust, bending and torsional oscillations were investigated both theoretically and experimentally when the wing encountered sinusoidal gust or random gust.

2. Response to Sinusoidal Gust

2.1. Theoretical Calculations

When an elastic wing encounters a gust w_G whose direction is normal to the chord, the wing is forced to deform. In this section the relations between sinusoidal fluctuations of gust and wing deformations are investigated.[3)]

The deformations depend not only on the time, but also on the position of the wing surface, and, accordingly, they have to be treated in the three-dimensional sense. However, since the modes of deformation can be classified into two types, i. e., the bending mode and the torsional mode, the following assumptions are made about the wing treated here:

1) Aerodynamic forces act on the wing two-dimensionally, or, in other words, the wing has a large aspect ratio, and the effects of the wing tip may be neglected.
2) The wing is restrained as a cantilever beam.

Furthermore, it is assumed that the flow is incompressible and inviscid.

If these assumptions are allowed, the equations of motion for the elastic wing may be given as follows:

$$\left.\begin{aligned} m\ddot{w}(y,t)-S_y\ddot{\theta}(y,t)+(EI)\frac{\partial^4 w(y,t)}{\partial y^4}&=L(y,t)\\ I_y\ddot{\theta}(y,t)-S_y\ddot{w}(y,t)-(GJ)\frac{\partial^2\theta(y,t)}{\partial y^2}&=M_y(y,t)\end{aligned}\right\} \tag{1}$$

where the system of co-ordinate axes is illustrated by Fig. 1, and m is the wing mass per unit span, I_y the moment of inertia (about the y axis), and S_y the static moment (about the y axis). These quantites are given as follows:

$$\left.\begin{aligned} m(y)&=\int_{chord}\rho_1(\xi,y)d\xi\\ S_y(y)&=\int_{chord}\rho_1(\xi,y)\xi d\xi\\ I_y(y)&=\int_{chord}\rho_1(\xi,y)\xi^2 d\xi\end{aligned}\right\} \tag{2}$$

In the above equations $\rho_1(\xi, y)$ is the wing mass per unit volume. $L(y, t)$ and $M_y(y, t)$, which are the terms of the right hand side of Eq. (1), are the lift

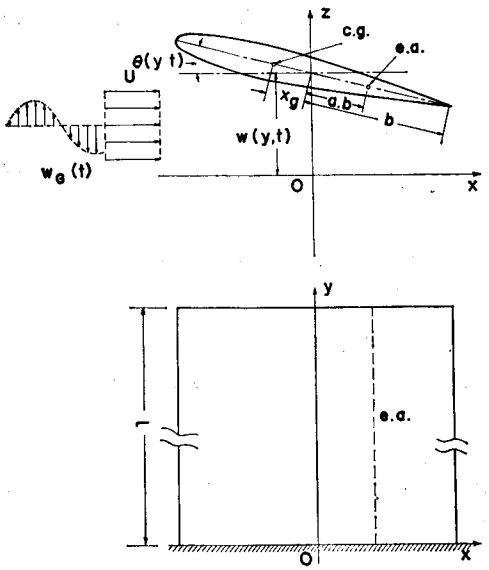

Fig. 1. Co-ordinate axes of elastic wing.

force and the pitching moment which act on the wing and are given by the following equations:

$$\left.\begin{aligned} L(y,t) &= L_g(t)+L_v(y,t) \\ &= (2\pi\rho bU)\left\{S(k)w_G(t)+C(k)\left[w(y,t)+U\theta(y,t)\right.\right. \\ &\qquad \left.\left.+b\left(\frac{1}{2}-a\right)\dot{\theta}(y,t)\right]\right\} \\ M_y(y,t) &= M_{yg}(t)+M_{yv}(y,t) \\ &= b\left(\frac{1}{2}+a\right)\left[L_g(t)+L_v(y,t)\right] \end{aligned}\right\} \qquad (3)$$

In order to obtain the response of a two-dimensional elastic wing to sinusoidal gust, it is necessary to solve Eq. (1), with the lift force and the pitching moment given by Eq. (3).

2.1.1. Derivation of the Solutions

Since the equations of motion (1) are expressed by fourth order simultaneous partial differential equations, it is difficult to solve them analytically. Therefore, the modes of oscillation were obtained by applying the solutions of the natural oscillation of a cantilever beam.

a) Bending Mode

In order to simplify the discussion, we have assumed that the bending mode and the torsional mode can be treated separately.

In the case of the bending deformation, the equation of motion is given as follows:

$$m\ddot{w}(y,t)+(EI)\frac{\partial^4 w(y,t)}{\partial y^4}=(2\pi\rho bU)[S(k)w_G(t)+C(k)\dot{w}(y,t)] \tag{4}$$

The boundary conditions are given by,

$$\left.\begin{aligned} &w(0,t)=\left.\frac{\partial w(y,t)}{\partial y}\right|_{y=0}=0 \\ &\left.\frac{\partial^2 w(y,t)}{\partial y^2}\right|_{y=l}=\left.\frac{\partial^3 w(y,t)}{\partial y^3}\right|_{y=l}=0 \end{aligned}\right\} \tag{5}$$

If both the gust $w_G(t)$ and the deformation $w(y,t)$ fluctuate sinusoidally, these quantities can be expressed as follows:

$$w_G(t)=\bar{w}_G e^{i\omega t},\quad w(y,t)=\bar{w}(y)e^{i\omega t} \tag{6}$$

Substituting Eq. (6) into Eq. (4), the following ordinary differential equation is obtained,

$$Aw''''(y)-\left[\left(\frac{k}{b}\right)^2+i\frac{B}{b^2}kC(k)\right]\bar{w}(y)=\frac{B}{b}\frac{\bar{w}_G}{U}S(k) \tag{7}$$

and the boundary conditions become

$$\left.\begin{aligned} &w(0)=w'(0)=0 \\ &w''(l)=w'''(l)=0 \end{aligned}\right\} \tag{8}$$

where

$$A=\frac{EI}{mU^2},\quad B=\frac{4\pi\rho b^2}{2m} \tag{9}$$

and A is the parameter of rigidity of the wing and B is the parameter of apparent mass.[4]

If the solution of Eq. (7) is expressed by the following series form,

$$\bar{w}(y)=\sum_{j=1}^{n} q_j\gamma_j(y) \tag{10}$$

where $\gamma_j(y)$ is the mode of natural oscillation of a cantilever beam and is given by

$$\begin{aligned}\gamma_j(y)=\gamma_0\{&[\cosh(k_jy)-\cos(k_jy)] \\ &+C[\sinh(k_jy)-\sin(k_jy)]\}\end{aligned} \tag{11}$$

and where γ_0, C are constants and k_j's are the roots of the following equation,

$$\cos(k_jl)\cosh(k_jl)=-1 \tag{12}$$

then, substituting Eq. (10) into Eq. (7), the following simultaneous equation is obtained.

$$\sum_{j=1}^{n}\left\{A\cdot\gamma_j''''(y_i)-\left[\left(\frac{k}{b}\right)^2+i\frac{B}{b^2}kC(k)\right]\gamma_j(k)\right\}q_j=\frac{B}{b}\frac{\bar{w}_G}{U}S(k) \tag{13}$$

where

$$y_i=\frac{il}{n}\quad (i=1, 2,\cdots\cdots, n)$$

b) Torsional Mode

In the case of the torsional mode, the method used in the case of the bending mode can also be applied. In this case the equation of motion is given by

$$I_y\ddot{\theta}(y, t)-(GJ)\frac{\partial^2\theta(y, t)}{\partial y^2}=b\left(\frac{1}{2}+a\right)(2\pi\rho bU)\times\left\{S(k)w_G(t)+b\left(\frac{1}{2}+a\right)C(k)\left[U\dot{\theta}(y, t)+b\left(\frac{1}{2}-a\right)\dot{\theta}(y, t)\right]\right\}\tag{14}$$

and the boundary conditions are

$$\theta(0, t)=0,\quad \left.\frac{\partial\theta(y, t)}{\partial y}\right|_{y=l}=0\tag{15}$$

Putting $\theta(y, t)=\bar{\theta}(y)e^{i\omega t}$, and

$$\bar{\theta}(y)=\sum_{j=1}^{n}p_j\nu_j(y)\tag{16}$$

then, the equation of motion can be rewritten by the following simultaneous equation:

$$\sum_{j=1}^{n}\left\{A'\nu_j''(y_i)+i\left(\frac{k}{b}\right)^2+B'\left(\frac{1}{2}+a\right)C(k)\left[1+ik\left(\frac{1}{2}-a\right)\right]\right\}\times\nu_j(y_i)p_j=-B'\left(\frac{1}{2}+a\right)S(k)\frac{\bar{w}_G}{U}\tag{17}$$

$$(i=1, 2,\cdots\cdots, n)$$

where

$$\nu_j(y)=\sin\left[\frac{(2j-1)\pi}{2l}y\right]\tag{18}$$

$$A'=\frac{GJ}{I_yU^2},\quad B'=\frac{4\pi\rho b^2}{2I_y}\tag{19}$$

and A' and B' are the parameters of torsional rigidity and apparent mass, respectively.

2.1.2. Some Examples of Calculations

Some examples of calculations of the bending mode and the torsional mode which were obtained by solving the simultaneous equations (13) or (17), are indicated in this section.

The calculations were, for the most part, carried out for the model wing which was used for the experiments. The physical properties and dimensions of the model wing are as follows:

half chord length: $b=60$ (mm)

span width: $l=500$ (mm)
elastic parameters: $EI=0.07$ (kg·m²), $GJ=0.054$ (kg·m²)
moments: $I_y=-0.0083$ (kg·s²), $S_y=-0.0034$ (kg·s²/m)
position of elastic axis: $a=-1/6$
uniform flow velocity: $U=10.0$ (m/s)
amplitude of gust velocity: $w_G/U=0.05$

a) Bending Mode

If j's are taken as 1, 2,……, 10, the roots of Eq. (12) are obtained as follows:

j	1	2	3	4	5
$k_j l$	1.875	4.694	7.855	10.996	14.137
j	6	7	8	9	10
$k_j l$	17.279	20.420	23.562	26.704	29.845

Using these values, the bending mode can be obtained by solving Eq. (13).

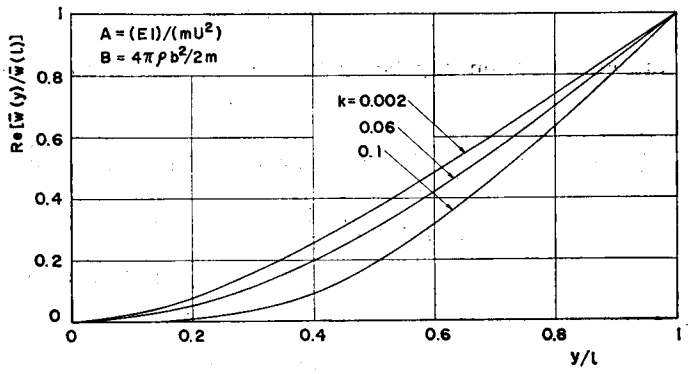

Fig. 2 (a). Bending mode.

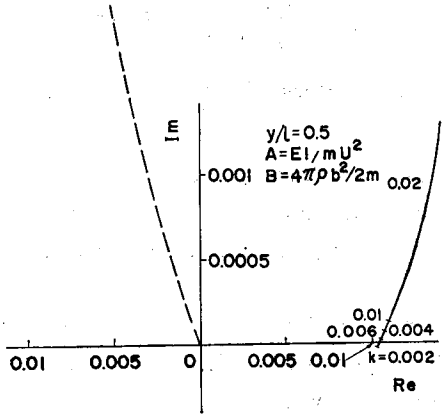

Fig. 2. (b) Phase characteristics of bending mode.

The real part of $\bar{w}(y)$ is illustrated in Fig. 2 (a), which is non-dimensionalized by the value at the wing tip ($y=l$). When the reduced frequency k is small, the fundamental mode is principal, but when k becomes large, the higher modes (until third mode) are contained. Fig. 2 (b) shows $\bar{w}(y)$, taking its real part as the horizontal axis and its imaginary part as the vertical axis. This figure shows that the phase difference between the deformation and the gust becomes large, when k becomes large, and that the imaginary part becomes positive at $k \geqq 0.004$. In this figure, the dotted line shows the limit at $k \to \infty$.

Next, the other examples of the results are illustrated by Fig. 3 (a) and Fig. 3 (b), when A is 0.01 and 0.1, and B is 0.01. This shows that the deformation $\bar{w}(y)$ becomes small when the rigidity of the wing increases. However, when k is small, the mode of deformation is not affected by the parame-

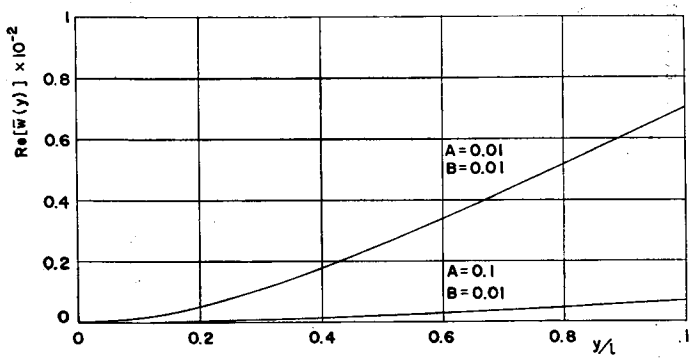

Fig. 3. (a) Bending mode (variation of parameters).

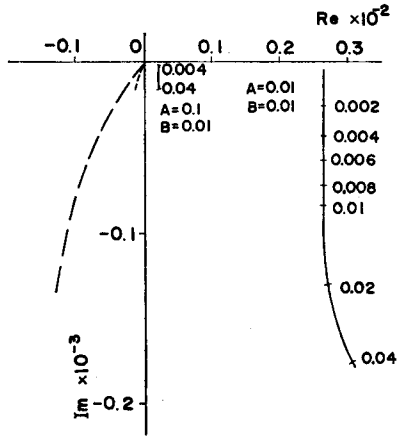

Fig. 3. (b) Phase characteristics of bending mode (variation of parameters).

ters A and B.

b) Torsional Mode

The torsional mode can be obtained by solving Eq. (17). The parameters A' and B' are -629.4 and -3.295, respectively, for the model wing. The real part is illustrated in Fig. 4 (a), which shows that the torsional mode contains only a few higher modes when k is small.

The phase difference, which is shown in Fig. 4 (b), has a tendency which is the same as in Sears' gust function. This indicates that the phase difference of the twisted angle follows the phase difference of the pitching moment which acts on the wing.

In this torsional case the modes of deformation do not change, if A' and B' change at a small value of k.

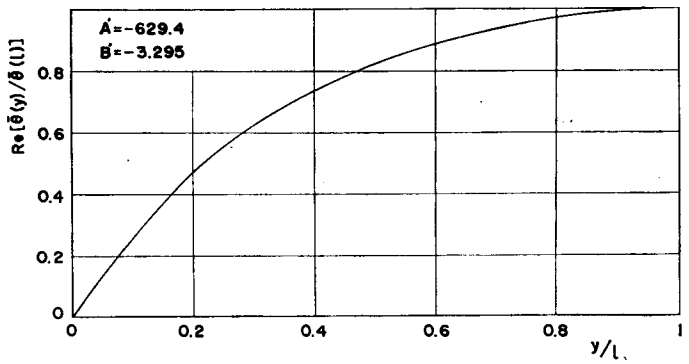

Fig. 4. (a) Torsional mode.

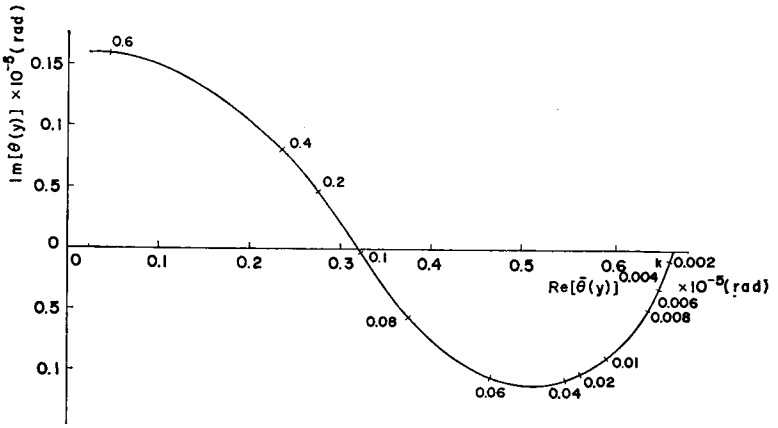

Fig. 4. (b) Phase characteristics of torsional mode ($A'=-629.4$, $B'=-3.295$).

2.2. Experiments

2.2.1. Experimental Apparatus

The experiments for obtaining the responses of a two-dimensional elastic wing were performed using the same apparatus which was used in the case of the rigid wing[1]. The side view of the apparatus is shown in Fig. 5.

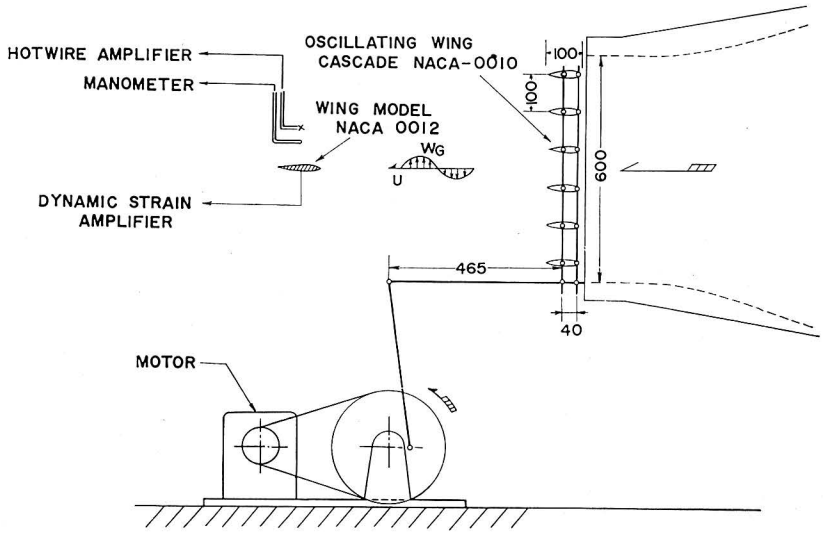

Fig. 5. Side view of apparatus.

In this case, however, the model wing was elastic, and had an NACA-0012 airfoil section; the chord length and the span width of this model wing were 120 mm and 500 mm, respectively. A duralmine plate (width 60 mm, thickness 1 mm) was used for the wing beam. A photograph is shown in Fig. 6.

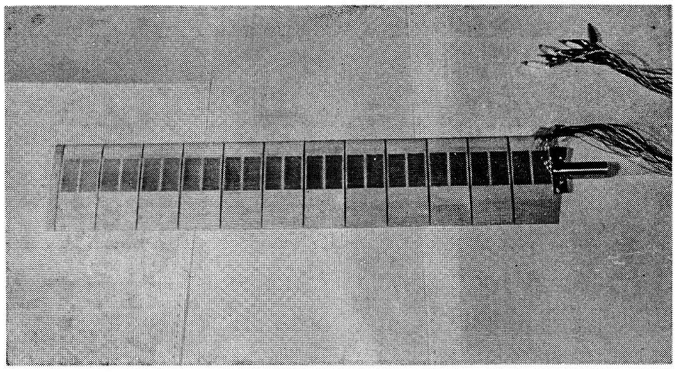

Fig. 6. Model wing.

This elastic wing was quite soft and was supported as a cantilever in the wind tunnel.

The responses of the wing (or the deformations of the wing) were me-

asured by strain gauges which were pasted on the wing beam at 4 points. These points are shown in Fig. 7. The mode of oscillation of the wing was also observed by the same strain gauges.

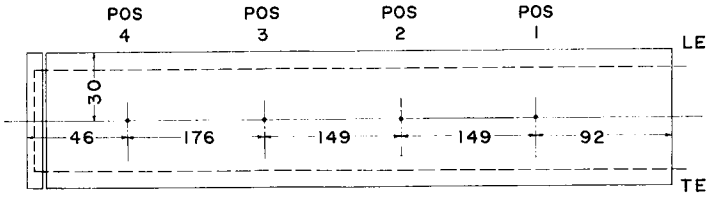

Fig. 7. Position of strain gauge.

The gust velocity was measured by a hot-wire anemometer with an x-type element. The outputs of these sensors were amplified and recorded by a photo-electric oscilloscope.

2. 2. 2. Experimental Results

a) Parameters

The parameters of the experiments are as follows:

angle of attack: $\alpha=0,\ 3,\ 6,\ 9°$

frequency of gust: $k=0.03,\ 0.04,\ 0.05,\ 0.06$

The velocity of the uniform flow, U, and the amplitude of the gust, $\bar{w}_G$, are constant, and are given by

$U=10.0$ (m/s)

$w_G/U=0.015$

b) Gust

Examples of the gust variations are shown in Fig. 8. This diagram shows that the gusts fluctuate sinusoidally.

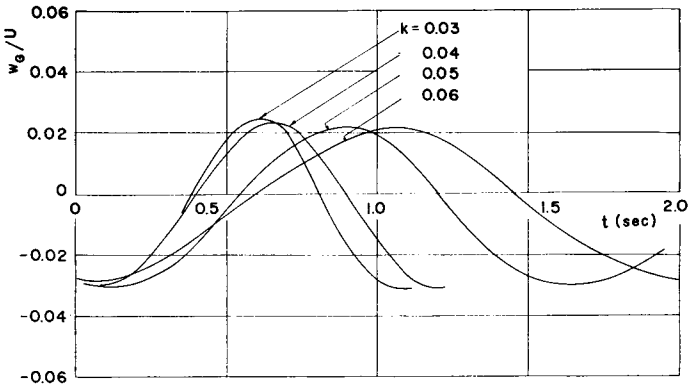

Fig. 8. Sinusoidal gust.

b) Bending Mode

The bending deformations of the model wing are shown in Fig. 9 (a) and Fig. 9 (b). The former shows the case in which the frequency of the gust is constant, and the latter the case in which the angle of attack is constant. These deformations are non-diensionalized by the value at the wing tip.

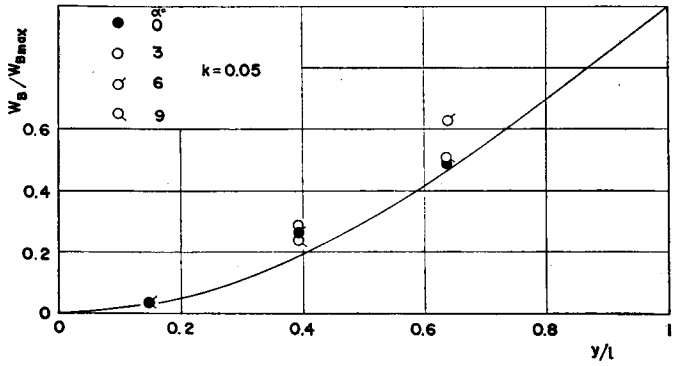

Fig. 9. (a) Bending mode (1).

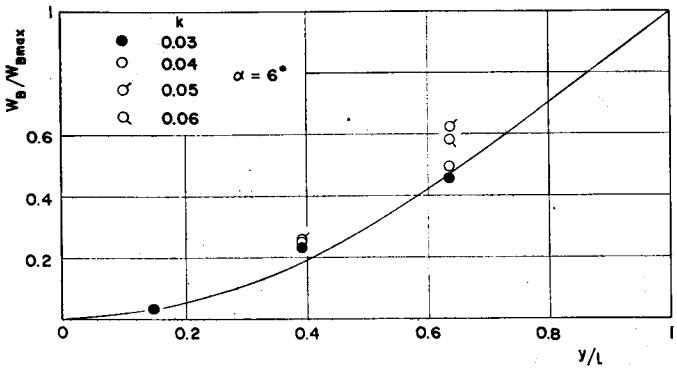

Fig. 9. (b) Bending mode (2).

These diagrams show that all values are not affected by the parameters A and B. In the same figure, the theoretical value which was obtained in 2.1.1. is illustrated with a solid line. The theoretical value agrees well with the experimental results.

c) Torsional Mode

In Fig. 10 (a) and Fig. 10 (b), the experimental results of the torsional modes are shown. The former shows the non-dimensionalized twisted angles in which the frequency of the gust is constant, and the latter the angles in which the angle of attack is constant.

Almost the same discussions can be presented for the torsional mode. In

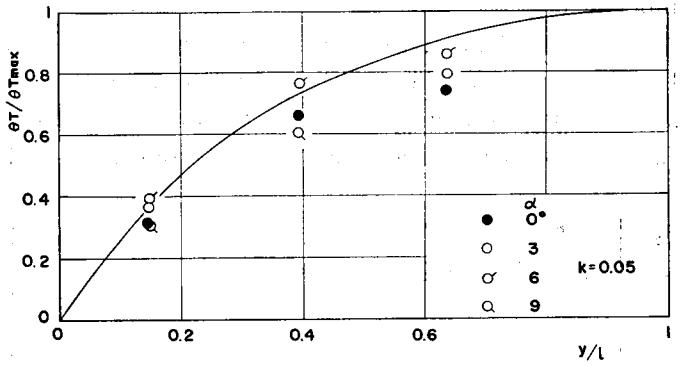

Fig. 10. (a) Torsional mode (1).

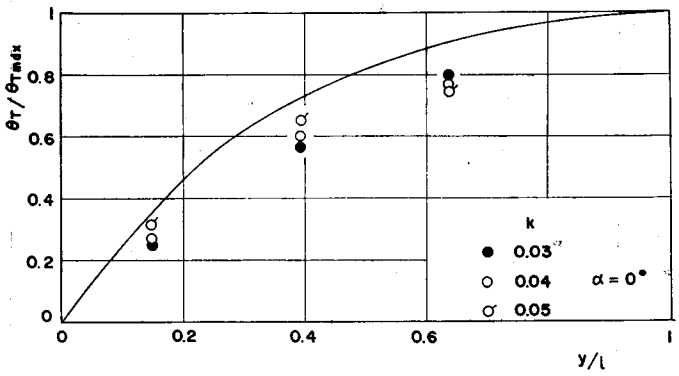

Fig. 10. (b) Torsional mode (2).

the same figure, the results of the theoretical calculations are illustrated with a solid line. Comparing this value with the experimental results, a small difference can be distinguished in this torsional case, especially in the neighborhood of the wing tip.

The principal reason for this difference may be that the experimental values do not contain a higher mode, but the theoretical values contain some higher modes of deformation. Also, it may be considered that an error caused by the position of the elastic axis occurs.

3. Response to Random Gust

3.1. Theoretical Calculations

In the preceding chapter, the responses of a two-dimensional elastic wing to a sinusoidal gust were investigated. In this chapter, the responses to a random gust are discussed.

Since the real gust which an airplane encounters in the atmosphere

generally varies randomly, this problem is considered to be very important.

In the case of sinusoidal gust, the modes of deformation of a wing can be obtained directly from the equations of motion, but the same method can not be used in the case of random gust, because the wing itself oscillates randomly. Accordingly, in the case of random gust, the deformation of the wing should be investigated by applying the method of a generalized harmonic analysis, i. e., the correlation function, power spectral density function, and frequency transfer function.

In addition to the assumptions given in the case of sinusoidal gust, it was assumed that random gust has no phase difference along the wing span, i. e., that the gust is an isotropic turbulence in a two-dimensional sense.

3. 1. 1. Case of Bending

Let us consider the frequency transfer function of the bending moment M which acts on the wing at y (Fig. 11). The bending moment M is given by the following equation,

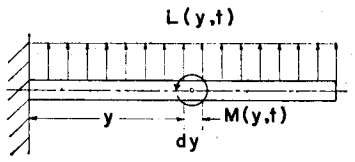

Fig. 11. Cantilever beam.

$$M(y, t)=\int_0^{l-y}(y+y_1)L(y+y_1, t)dy_1 \tag{20}$$

Taking the ensemble average with t, the auto-correlation function of $M(y, t)$ can be obtained as follows:

$$R_M(y, \tau)=\int_0^{l-y}\int_0^{l-y'}(y+y_1)(y'+y_1')R_L(y+y_1, y'+y_1', \tau)dy_1dy_1' \tag{21}$$
$$(y'\to y)$$

It was assumed that the lift force $L(y, t)$ could be expressed by superimposing two kinds of lift forces, i. e., one by the gust and the other by the oscillation of the wing.

$$L(y, t)=L_g(t)+L_v(y, t) \tag{22}$$

where $L_g(t)$ and $L_v(y, t)$ can be obtained, if the influence functions g and v are known.

$$\left.\begin{aligned} L_g(t)&=\int_{-\infty}^{\infty}g(t')w_G(t-t')dt' \\ L_v(y, t)&=\int_0^y dy'\int\int_{-\infty}^{\infty}v(t, |\eta-y'|)w(t-t', \eta)dt'd\eta \end{aligned}\right\} \tag{23}$$

Therefore, the auto-correlation function of the lift force can be reduced in

the same manner as in the case of a bending moment.

$$R_L(y, y', \tau) = R_{Lg}(\tau) + R_{Lv}(y, y', \tau) \tag{24}$$

Substituting Eq. (24) into Eq. (21), and performing a Fourier transformation on both sides, the power spectral density function of the bending moment is expressed by the following equation.

$$\Phi_M(y, k) = \int_0^{l-y}\int_0^{l-y'} dy_1 dy_1' \cdot (y+y_1)(y'+y_1') \times [\Phi_{Lg}(k) + \Phi_{Lv}(y+y_1, y'+y_1', k)] \tag{25}$$

In this equation the unknown functions, Φ_{Lv} and Φ_{Lg}, can be obtained from the equation of motion of the wing and Eq. (23) in the following manner.

If the wing shows bending deformation only, the equation of motion is rewritten as follows:

$$m\ddot{w}(y, t) + (EI)\frac{\partial^4 w(y, t)}{\partial y^4} = \int_{-\infty}^{\infty} g(t') w_G(t-t') dt' + \int_0^y dy' \iint_{-\infty}^{\infty} v(t', |\eta - y'|) w(t-t', \eta) dt' d\eta \tag{26}$$

Furthermore, it was assumed that $w(y, t)$ could be expressed by the products of the time-depending term and the position-depending term, i. e.,

$$w(y, t) = \gamma(y) q(t) \tag{27}$$

Multiplying both sides of Eq. (26) by $q(t+\tau)$, and taking the ensemble average, the differential equation of the auto-correlation function of $q(t)$ can be obtained as follows:

$$m\gamma(y)\frac{d^2}{d\tau^2} R_q(\tau) + (EI)\gamma''''(y) R_q(\tau) = \int_{-\infty}^{\infty} g(t') R_{qw_G}(\tau - t') dt + \int_0^y dy' \iint_{-\infty}^{\infty} v(t', |\eta - y'|) \gamma(\eta) \frac{d}{d\tau} R_q(\tau - t') dt' d\eta \tag{28}$$

where the relations between the derivatives of the auto-correlation function, such as

$$\overline{q(t)\ddot{q}(t+\tau)} = \frac{d^2}{d\tau^2} R_q(\tau) \quad \text{etc.} \tag{29}$$

are used.

Through Fourier transformation on both sides of Eq. (28), the relation between the power spectral density functions can be reduced as follows:

$$-m\gamma(y)k^2 \Phi_q(k) + (EI)\gamma''''(y)\Phi_q(k) = \int_{-\infty}^{\infty} g(t') e^{-ikt'} dt' \cdot \Phi_{qw_G}(k)$$

$$+\int_0^y dy' \iint_{-\infty}^{\infty} v(t', |\eta - y'|) \gamma(\eta) e^{-ikt'} [ik\Phi_q(k)] dt' d\eta \tag{30}$$

To obtain the power spectral density function of the deformation $\Phi_q(k)$, it is necessary that $\Phi_{qw_G}(k)$ be known. In order to obtain $\Phi_{qw_G}(k)$, the relation between $\Phi_{qw_G}(k)$ and $\Phi_{w_G}(k)$ can be reduced by the same process as in Eq. (30).

$$\begin{aligned} &-m\gamma(y)k^2\Phi_{qw_G}(k) + (EI)\gamma''''(y)\Phi_{qw_G}(k) \\ &= \int_{-\infty}^{\infty} g(t') e^{ikt'} dt' \cdot \Phi_{w_G}(k) \\ &+ \int_0^y dy' \iint_{-\infty}^{\infty} v(t', |\eta - y'|) \gamma(\eta) e^{ikt'} [-ik\Phi_{qw_G}(k)] dt' d\eta \end{aligned} \tag{31}$$

From Eq. (30) and Eq. (31), $\Phi_q(k)$ can be expressed by the power spectral density function of the gust $\Phi_{w_G}(k)$ as follows:

$$\Phi_q(k) = \left| \frac{S_1(k)}{m\gamma(y)k^2 - (EI)\gamma''''(y) + ikC_0(y, k)} \right|^2 \Phi_{w_G}(k) \tag{32}$$

where

$$\left.\begin{aligned} S_1(k) &= \int_{-\infty}^{\infty} g(t') e^{-ikt'} dt' \\ C_0(y, t) &= \int_0^y dy' \iint_{-\infty}^{\infty} v(t', |\eta - y'|) e^{-ikt'} dt' d\eta \end{aligned}\right\} \tag{33}$$

Accordingly, $\Phi_{L_q}(k)$ and $\Phi_{L_v}(y, y'; k)$ can be obtained from Eq. (23) as follows:

$$\Phi_{L_q}(k) = \iint_{-\infty}^{\infty} g(t_1) g(t_2) e^{ik(t_1 - t_2)} dt_1 dt_2 \cdot \Phi_{w_G}(k) \tag{34}$$

$$\begin{aligned} \Phi_{L_v}(y_1, y_2, k) = &- \int_0^{y_1} dy_1' \int_0^{y_2} dy_2' \cdot \iiint\int_{-\infty}^{\infty} v(t_1', |\eta_1 - y_1'|) v(t_2', |\eta_2 - y_2'|) \\ &\times \gamma(\eta_1)\gamma(\eta_2) e^{ik(t_1' - t_2')} dt_1' dt_2' \cdot d\eta_1 d\eta_2 \cdot k^2 \cdot \Phi_q(k) \end{aligned} \tag{35}$$

With the above relations, the power spectral density function of the bending moment at an arbitrary point y can be obtained. Furthermore, the frequency transfer function $T_M(k)$, which is defined as

$$T_M(k) = \Phi_M(k) / \Phi_{w_G}(k) \tag{36}$$

can also be obtained readily with Eq. (25).

3.1.2. Case of Torsion

Next, the power spectral function and the frequency transfer function of the torsional moment T, which act on the wing at an arbitrary point y, can still be obtained in the same manner as in the case of the bending moment.

In this case, the equation of motion is given by

$$I_v \ddot{\theta}(y, t) - (GJ) \frac{\partial^2 \theta(y, t)}{\partial y^2} = M_v(y, t) \tag{37}$$

and the pitching moment is assumed to be expressed as follows:

$$\begin{aligned} M_y(y, t) &= M_{y_g}(t) + M_{y_v}(y, t) \\ &= b\left(a+\frac{1}{2}\right) L_g(t) + \int_0^y dy' \int\int_{-\infty}^{\infty} [u_1(t', |\eta - y'|)\theta(t-t', \eta) \\ &\quad + u_2(t', |\eta - y'|)\dot{\theta}(t-t', \eta)] dt' d\eta \end{aligned} \tag{38}$$

where u_1 and u_2 are the influence functions.

Since the processes for reducing the power spectral function and the frequency transfer function were the same as in the case of bending, only the results of calculation were expressed without reduction.

First, the power spectral density function of the twisted angle was obtained as follows:

$$\Phi_p(y, k) = \left| \frac{b\left(a+\frac{1}{2}\right) S_1(k)}{I_y \nu(y) k^2 + (GJ)\nu''(y) + C_1(y, k) + ikC_2(y, k)} \right|^2 \Phi_{wG}(k) \tag{39}$$

where

$$\left.\begin{aligned} C_1(y, k) &= \int_0^y dy' \int\int_{-\infty}^{\infty} u_1(t', |\eta - y'|)\nu(\eta) e^{-ikt'} dt' d\eta \\ C_2(y, k) &= \int_0^y dy' \int\int_{-\infty}^{\infty} u_2(t', |\eta - y|)\nu(\eta) e^{-ikt'} dt' d\eta \end{aligned}\right\} \tag{40}$$

Next, the power spectral density function of the torsional moment $\Phi_T(y, k)$ was obtained as follows:

$$\Phi_T(k) = \int_0^y \int_0^{y'} dy dy' \cdot [\Phi_{My_g}(k) + \Phi_{My_v}(y, y', \tau)] \tag{41}$$

Therefore, the frequency transfer function can be obtained by

$$T_T(k) = \Phi_T(k) / \Phi_{wG}(k) \tag{42}$$

3.1.3. Some Examples of Calculations

Using the relations obtained in the previous sections, the responses to random gust can be calculated. In this section, some results of calculations for the model wing will be indicated. Furthermore, the results of calculations for wings of different rigidity will also be given.

However, the modes of deformation, $\tau(\eta)$ and $\nu(\eta)$, and the influence functions, g, v, u_1 and u_2, are all unknown quantities. Therefore, $S_1(k)$, $C_0(y, k)$, $C_1(y, k)$, and $C_2(y, k)$ are also unknowns. Accordingly, these quantities were assumed to be as follows:

First, the fundamental mode of natural oscillation of a cantilever beam was used for $\tau(\eta)$ and $\nu(\eta)$, i.e., $\tau_1(\eta)$ of Eq. (11) in 2.1.1. was substituted for $\tau(\eta)$ and $\nu_1(\eta)$ of Eq. (18) for $\nu(\eta)$. Next, Sears' gust function and Theodorsen's function were used for $S_1(k)$ etc.[5], i.e.,

$$\left.\begin{aligned} S_1(k) &= (2\pi\rho bU)S(k) \\ C_0(y,\ k) &= (2\pi\rho bU)\gamma(y)C(k) \\ C_1(y,\ k) &= (2\pi\rho bU^2)\nu(y)C(k)\left[b\left(a+\frac{1}{2}\right)\right] \\ C_2(y,\ k) &= (2\pi\rho bU)\nu(y)C(k)\left[b^2\left(\frac{1}{4}-a^2\right)\right] \end{aligned}\right\} \tag{43}$$

Substituting these quantities into the equations in 3.1.1. and 3.1.2., the frequency transfer function of the bending deformation, $T_q(y,\ k)$, and that of the twisted angle by torsion, $T_p(y,\ k)$, can be obtained. The frequency transfer functions of the bending moment and the torsional moment can also be obtained.

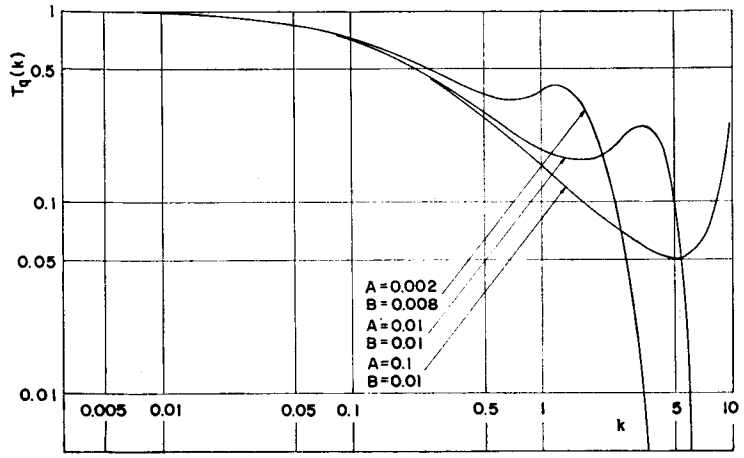

Fig. 12. Frequency transfer functions of deformation by bending.

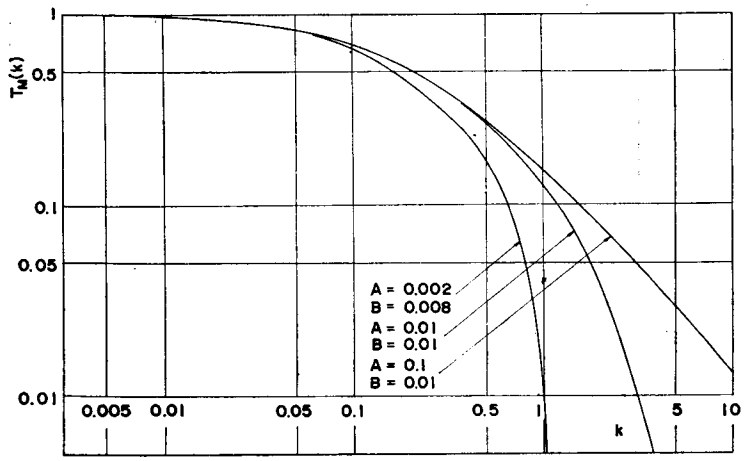

Fig. 13. Frequency transfer functions of bending moment.

In the case of bending the results of calculations are shown in Fig. 12, $(T_q(k))$, and Fig. 13, $(T_M(k))$. In these figures, A is taken as the parameter, while B is constant. The curve of $A=0.002$ and $B=0.008$ shows the case of the model wing.

From these figures, the frequency transfer functions are seen to be affected by the parameters A and B. Specifically, B affects the inclination of decline of the frequency transfer function when k is large, and A affects the degree of decline. Furthermore, it is shown that the frequency transfer function of the bending moment decreases earlier than that of the deformation.

Next, in the case of torsion, the results are shown in Fig. 14, $(T_p(k))$, and Fig. 15, $(T_T(k))$. In this case, it is also shown that almost the same discus-

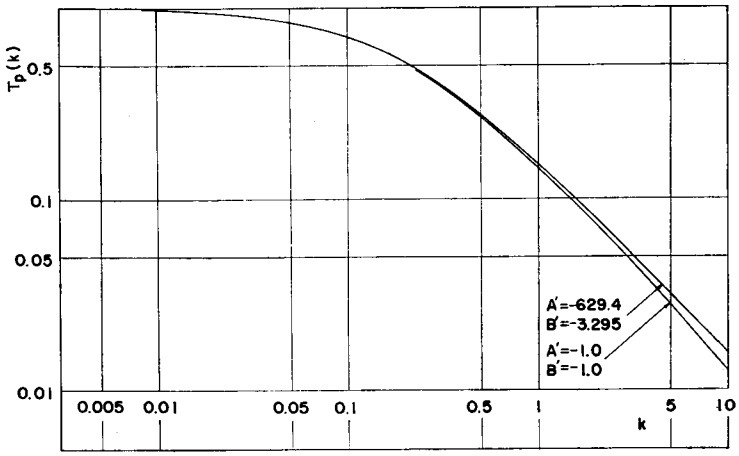

Fig. 14. Frequency transfer functions of twisted angle.

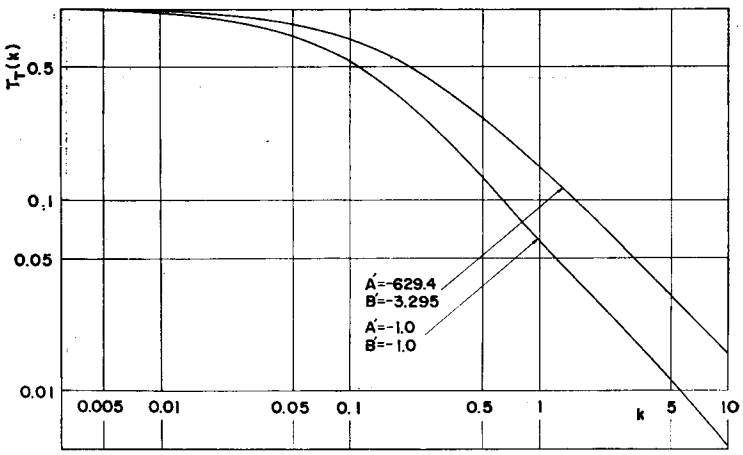

Fig. 15. Frequency transfer functions of torsional moment.

sions as in the case of bending can be given, but the inclination of decline is milder than in the case of bending.

3.2. Experiments

3.2.1. Experimental Apparatus

The responses of an elastic wing to random gust were measured with the same apparatus used in the experiments with the rigid wing[1].

The random gust was induced by a coarse grid, which was placed in the uniform flow of a wind tunnel. The grid members were made of bars with a circular section of 20 mm diameter; the gauge of the mesh of the grid was 4.5. This gusty wind may be regarded as an isotropic turbulence, and the power spectra will be shown later.

In this case, the experimental data were recorded on magnetic tape with a tape recorder, and the analogue quantities were converted to digital ones by a high speed sampling A-D converter, and the resulting calculations were executed by a digital computer. The block diagram of the measurements is shown in Fig. 16.

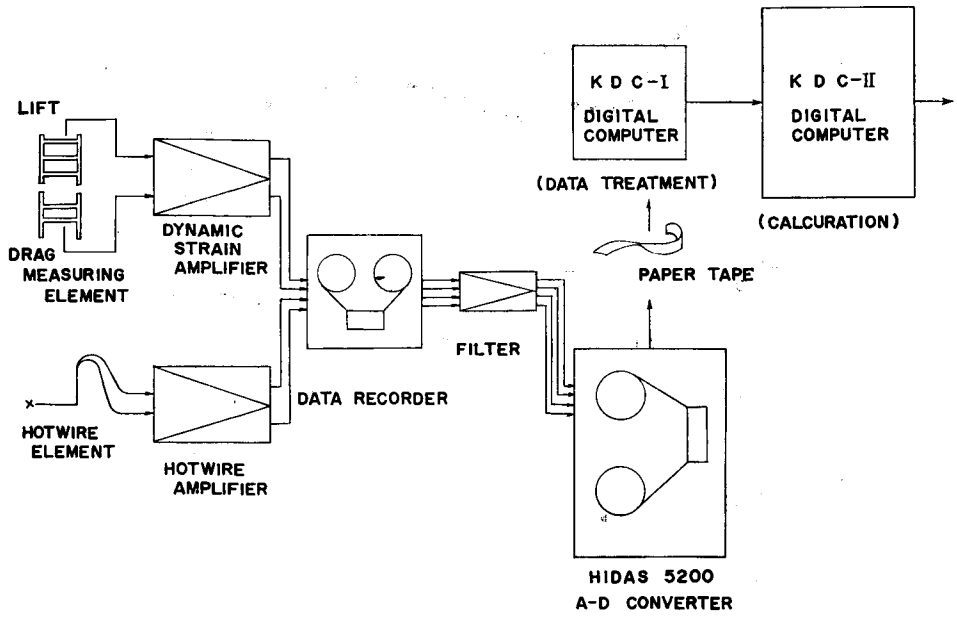

Fig. 16. Block diagram.

3.2.2. Experimental Results

The parameter of this case is the variation of the initial angle of attack of the model wing. In our experiment, it was varied from 0, 3, 6, to 9°. The

uniform flow velocity was approximately constant, about 10 m/s.

The equations for calculating the correlation functions, the power spectral density functions, and the frequency transfer functions are given as follows:

a) Auto-correlation function:

$$R_y(\tau) = \sum_{i=1}^{N} y(t_i)y(t_i+\tau) \tag{44}$$

b) Power spectral density function:

$$\Phi_y(k) = \int_0^\infty R_y(\tau)\cos(k\tau)d\tau \tag{45}$$

c) Frequency transfer function:

$$T_y(k) = \Phi_y(k)/\Phi_{wg}(k) \tag{46}$$

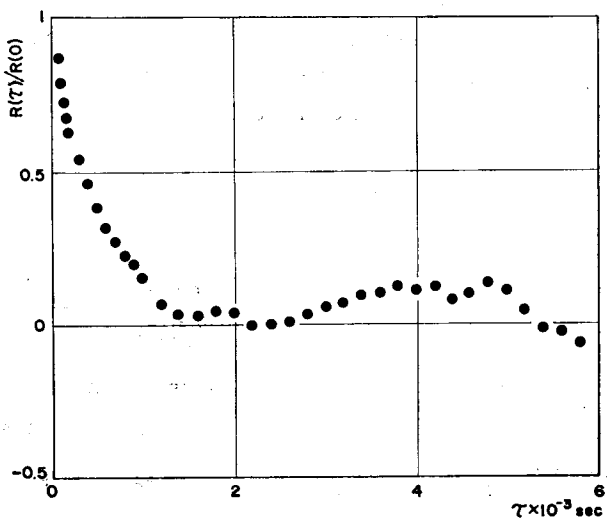

Fig. 17. (a) Correlation of gust.

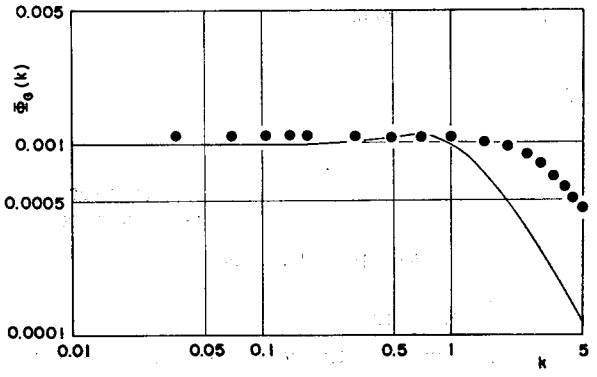

Fig. 17. (b) Power spectrum of gust.

In the following discussions, the auto-correlation functions $R(\tau)$ were normalized by dividing by $R(0)$, which is equal to the mean square value.

a) Gust

The auto-correlation function and power spectral density function of the present random gust are shown in Fig. 17 (a) and Fig. 17 (b), respectively. These functions were almost the same as the case of the rigid wing[1], but the power spectral density function did not agree well with the theoretical value of the isotropic turbulence at a higher frequency.

b) Bending

The auto-correlation functions and the power spectral density functions of deformation by the bending moment are shown in Fig. 18 (a) and Fig. 18 (b), respectively. The point measured on the wing was POS 1, and the angle of attack was taken as the parameter.

These figures show that both the auto-correlation functions and the power

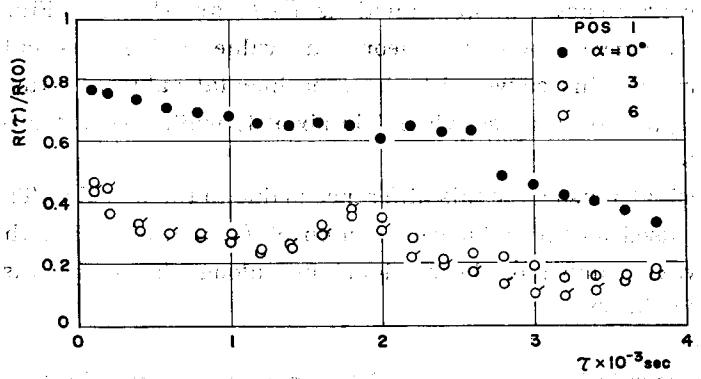

Fig. 18. (a) Correlations of bending moment.

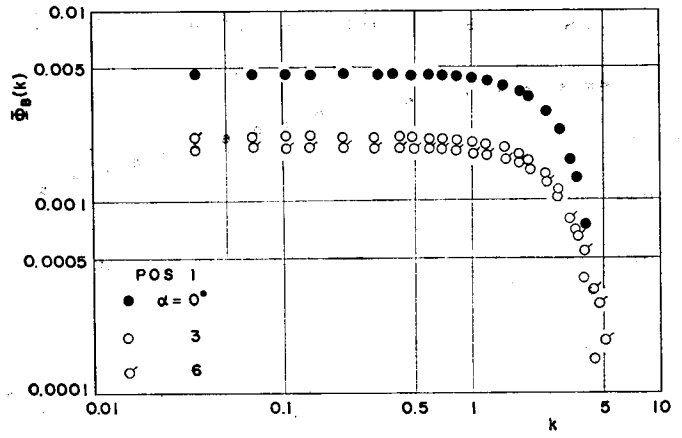

Fig. 18. (b) Power spectra of bending moment.

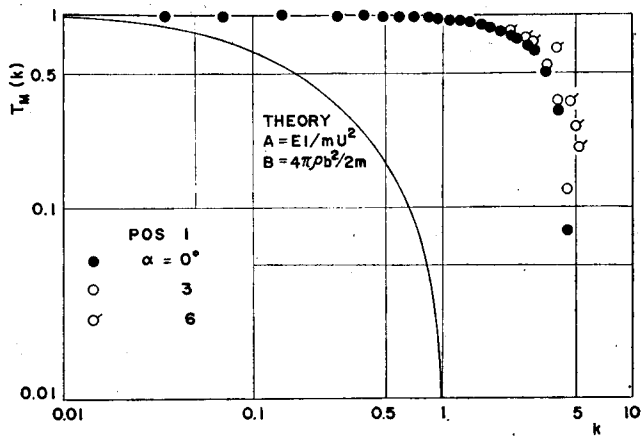

Fig. 18. (c) Frequency transfer functions of bending moment.

spectral density functions decrease rapidly in the neighborhood of $k=5$.

Next, the frequency transfer functions $T_M(k)$ are shown in Fig. 18 (c). In this figure, the curve shows the theoretical value which was calculated in 3.1.3. Comparing this curve with the experimental values, it was found that the former begins to decrease when k is about 1, while the latter is flat until k is nearly 4.

The principal reason for this difference is due to the fact that Theodorsen's function was used as the influence function of L_v, and also that the distribution of the wave number of the random gust along the span was not considered in the theory.

c) Torsion

The auto-correlation functions and the power spectral density functions of the deformation by torsion are shown in Fig. 19 (a) and Fig. 19 (b), respectively. The same discussions as in the bending moment are still valid in this

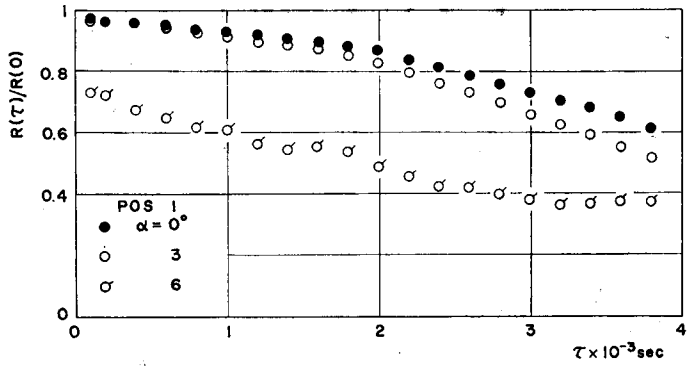

Fig. 19. (a) Correlations of torsional moment.

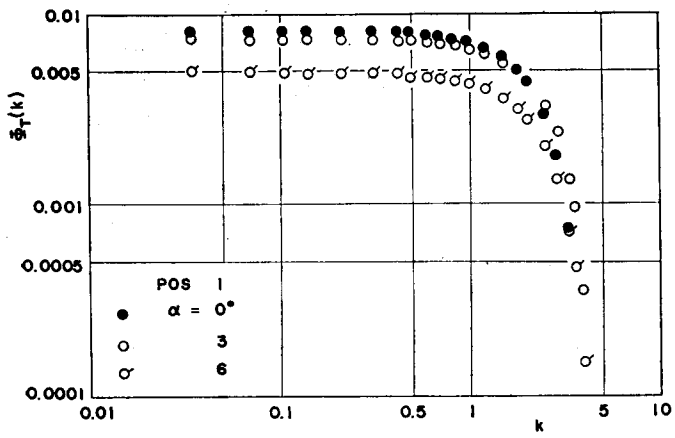

Fig. 19. (b) Power spectra of torsional moment.

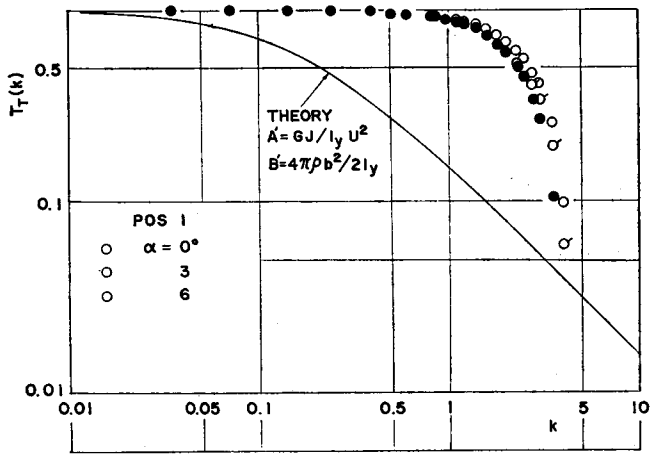

Fig. 19. (c) Fequency transfer functions of torsional moment.

case.

The frequency transfer functions are shown in Fig. 19 (c). The difference between the theoretical result and the experimental result in this case appears to be due to the fact that the inclination of decline with k differs between the experimental and theoretical cases.

One of the reasons for this difference is due to the fact that the frequency transfer function is affected by the position of the elastic axis.

4. Conclusion

The responses of the two-dimensional elastic wing to sinusoidal gust and random gust were investigated, and the results of the theoretical calculations

were compared with the experimental values. The gusts treated in this report are only those components normal to the uniform flow.

The deformations of the elastic wing are divided into two types, i.e., deformation by bending, and deformation by torsion, the non-steady effects were taken into consideration for each deformation.

For the case of sinusoidal gust, the equations of motion were solved directly by applying the solutions for the harmonic oscillation of a cantilever beam. The theoretical values agreed well with the experimental values in this case.

For the case of random gust, the method of generalized harmonic analysis was applied. The frequency transfer functions from the theoretical calculations were compared with those from the experimental values. In the case of bending, the experimental and theoretical values of the reduced frequency, k, at which the transfer functions begin to decrease, did not agree. In the case of torsion, the inclination of decline of the theoretical results differ from that of the experimental values. However, the reasons for these differences are due to the following facts:

1) The parameters, A, B or A', B', in the theory differed from the values in the experiments.
2) The phase difference of the gust along the wing span was not considered in this report.

5. References

1) Maeda, H., Kobayakawa, M., "Studies on the Gust Response of a Wing, Part 1 Response of a Two-Dimensional Rigid Wing", *Memo, Faculty Eng. Kyoto Univ.*, Vol XXXII, Part 4, October, 1970.
2) Bispringhoff, R. L., Ashley, H., Halfmann, R. L., *Aeroelasticity*, Addison-Wesley Pub. Co. Inc., 1955.
3) Goland, M. G., Luke, Y. L., "A Study of the Bending-Torsion Aeroelastic Modes for Aircraft Wings, *J. A. S.*, Vol. 16, No. 7, July, 1949.
4) Sears, W. R., Sparks, B. O., "On the Reaction of an Elastic Wing to Vertical Gusts", *J. A. S.*, Vol. 7, No. 2, December, 1941.
5) Hakkinen, R. J., Richardson, A. S., "Theoretical and Experimental Investigation of Random Gust Loads: Part I. Aerodynamic Transfer Function of a Simple Wing Configuration in Incompressible Flow", *NACA Tech.* part of Journal name TN 3878, 1957.

6. Notations

a: position of elastic axis
A, A': parameters of wing rigidity
B, B': parameters of apparent mass
b: half chord length

$C(k)$, $S(k)$: Theodorsen's function and Sears' function
EI : rigidity of bending
GJ : rigidity of torsion
k, k_j : reduced frequency and roots of Eq. (12)
L, M_y : lift and pitching moment
l : span width of wing
m : wing mass
I_y, S_y : moment of inertia and static moment
w : deformation by bending
θ : deformation by torsion
U, w_G : uniform flow velocity and gust velocity
$R(\tau)$: correlation function
$\Phi(k)$: power spectral density function
$T(k)$: frequency transfer function
$g(t')$: influence function of gust
v, v_1, v_2 : influence functions of deformation